An Optical Multicast Overlay Scheme Using Optical Sub-Carriers for WDM Passive Optical Networks

Yang Qiu, *Student Member,* and Chun-Kit Chan, *Senior Member, IEEE,*

Abstract—**We propose to make use of optical sub-carriers to realize optical multicast overlay on a WDM passive optical network. By employing optical carrier suppression technique at each downstream optical transmitter at the OLT, two coherent optical sub-carriers are generated to carry the 10-Gb/s downstream unicast DPSK signal and the 10-Gb/s downstream multicast ASK signal, separately without any additional light sources. At the ONU, the 10-Gb/s upstream data is superimposed on the received downstream unicast DPSK signal, to form the upstream ASK signal. System characterization is performed to optimize the performance. In addition, we further demonstrate simultaneous optical overlay of two streams of multicast data in the network.**

Index Terms—**wavelength-division-multiplexing, passive optical network, orthogonal modulation, differential phase shift keying, amplitude shift keying, multicast, optical carrier suppression, sub-carrier modulation.**

I. Introduction

THE WAVELENGTH-division-multiplexed passive optical network (WDM-PON) is regarded as a promising approach to deliver high speed services to both business and residential subscribers. Common WDM-PONs support two-way point-to-point data transmission between the optical line terminal (OLT) and the individual subscribers, via the respective designated set of wavelengths. However, with more diverse multimedia and data services available for broadband access nowadays, the access network has to be flexible enough to cope with various different modes of data or video delivery such as broadcast and multicast, in addition to unicast transmissions. Hence, the same data or video service can be delivered to a designated subset of subscribers or optical network units (ONUs), and the connections can also be flexibly reconfigured at the OLT.

Multicast transmission in a WDM-PON significantly enhances the network resource utilization efficiency for multiple destination traffic and improves the cost effectiveness. Optical multicast can be realized by establishing one-to-many lightpaths on the optical layer, and thus reduces the loading of the electronic network processors or routers on the network layer and achieves much higher processing speed. In order to realize optical multicast overlay on a WDM-PON, two crucial features have to be carefully designed, namely how to overlay the multicast traffic to the existing network infrastructure which is carrying the two-way point-to-point traffic, as well as the overlay control technique for connection reconfiguration.

Recently, several interesting schemes [1-9] have been proposed to optically overlay the multicast data onto the existing point-to-point or unicast wavelengths in WDM-PONs, using various feasible and practical optical signal processing techniques. The common principle is to selectively enable or disable the broadcast service superimposed on each downstream wavelength at the OLT, such that only the designated subset of ONUs can properly retrieve the broadcast service. Hence, optical multicast is realized without any additional dedicated light source for the multicast service.

In [1-6], the multicast data in either differential phase-shift keying (DPSK) format [1-3], inverse-return-to-zero (IRZ) format [4], or subcarrier-multiplexed (SCM) form [5,6], were modulated onto all downstream unicast wavelengths, each of them were carrying its unicast non-return-to-zero (NRZ) amplitude-shift keying (ASK) data. The superimposed multicast data could be enabled or disabled by setting low or high value in the extinction ratio [2,4-6] of the unicast ASK data, respectively, or switching the unicast data format between IRZ and NRZ [1], respectively. In [3], the multicast DPSK data superimposed on a particular downstream unicast IRZ wavelength could be disabled by applying temporal delay to the respective downstream unicast data so as to induce excessive temporal bit misalignment between the two data streams. In general, for the wavelengths under multicast-disabled state, their respective superimposed multicast signal would suffer from severe intensity fluctuation and thus could not be properly demodulated or detected at the destined ONUs. However, the downstream unicast ASK data might also suffer from system penalty due to its reduced extinction ratio under multicast-enabled state. Another approach [7] employed double-sideband DPSK format for the downstream unicast data, while the central carrier was extracted to carry the multicast ASK data. The multicast data on a particular wavelength could be disabled by suppressing its optical carrier at the OLT. However, double-sideband DPSK suffers from serious coherent beating noise and requires additional electric low-pass filter at the ONU for multicast data reception.

In [8,9], instead of superimposing the multicast data onto the unicast data on each downstream wavelength, the out-

Manuscript received 15 August 2009; revised 23 January 2010. This work was supported in part by a research grant from Hong Kong Research Grants Council (Project No. CUHK4105/08E).

The authors are with the Department of Information Engineering, The Chinese University of Hong Kong, Shatin, N. T., Hong Kong, China e-mail: (qy007@ie.cuhk.edu.hk; ckchan@ie.cuhk.edu.hk).

Digital Object Identifier 10.1109/JSAC.2010.100807.

0733-8716/10/$25.00 © 2010 IEEE

Authorized licensed use limited to: Chinese University of Hong Kong. Downloaded on July 26,2010 at 16:13:08 UTC from IEEE Xplore. Restrictions apply.

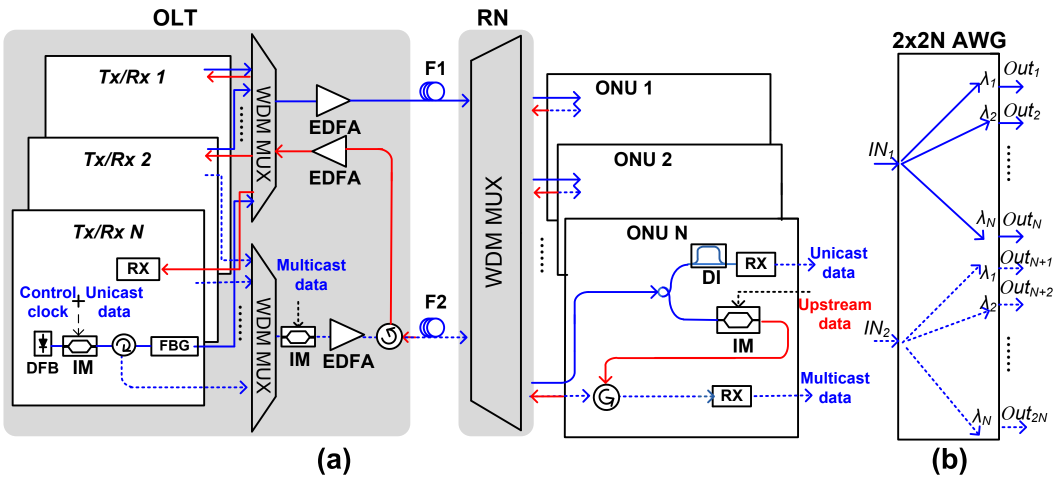

Fig. 1. A WDM-PON with proposed optical multicast overlay scheme, (b) a typical periodic 2 × 2N AWG used as the WDM MUX at RN. F1 & F2: fiber feeders, FBG: fiber Bragg grating, IM: optical intensity modulator, EDFA: Erbium doped fiber amplifier, DI: delay interferometer.

put power from each transmitter at the OLT was split into two parts. One of them was modulated with the respective downstream unicast data before being delivered to its destined ONU. the other unmodulated portion was combined with those from the other transmitters at the OLT before being commonly modulated with the multicast data. Thus, no additional dedicated light source for the multicast data was needed. The two streams were routed to the remote node (RN) via different fiber feeders. The control of the multicast transmission on individual was achieved either by controlling the input polarization state of the unmodulated power to the common optical modulator for multicast data modulation [8] or by on/off switching of the unmodulated power, via an optical ON/OFF switch [9].

Recently, we proposed and demonstrated a novel optical multicast overlay scheme [10] which can guarantee the performance and alleviate the possible Rayleigh backscattering effect. It was based on the optical carrier suppression (OCS) technique [11] at the OLT so as to generate the optical subcarriers or sidebands for multicast ASK data modulation. The downstream unicast data was modulated in DPSK format, which would be re-modulated with the upstream ASK data at the respective destined ONU. The control of the multicast transmission was achieved by simply setting the control clock signal at the OLT. Simultaneous 10-Gb/s operations for downstream and upstream unicast traffic, as well as downstream multicast traffic were demonstrated with satisfactory performance. In this paper, we further investigated and optimized the performance of this optical sub-carrier based optical multicast overlay scheme with relaxed clock requirement for the OCS process. In addition, we further enhance the network functionality by overlaying two multicast data streams over the WDM-PON by mean of ASK/DPSK orthogonal modulation on the optical source signal for multicast transmission.

This paper is organized as follows. Section II describes the network architecture, the operation principles of the proposed optical sub-carrier based optical multicast overlay scheme and its experimental demonstration. Section III describes the modified version of our scheme and its performance improvement. Section IV discusses the requirement of the control clock frequency for OCS and the characterization of possible residual Rayleigh backscattering in the network. Section V presents the technique and the experimental demonstration of overlaying two multicast data streams over the WDM-PON. Section VI summarizes the paper.

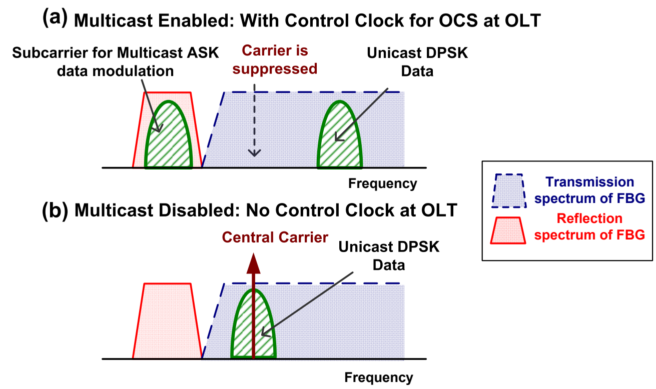

Fig. 2. Spectra of downstream carrier to illustrate the principle of multicast overlay control via optical carrier suppression (OCS).

II. WDM-PON WITH PROPOSED OPTICAL SUB-CARRIER BASED MULTICAST OVERLAY SCHEME

Fig. 1(a) depicts a WDM-PON with N ONUs. At the OLT, the CW light from each transmitter is first modulated by a composite signal, which comprises a sinusoidal control clock signal and the downstream unicast NRZ data, via a Mach-Zehnder optical intensity modulator (IM), biased at its null transmission point. The peak-to-peak driving voltage (V_{pp}) of both the control clock and the unicast data should be twice of the half-wave voltage (V_π) of the IM. In this way, the optical central carrier is suppressed, while the two generated sidebands (optical sub-carriers) are carrying the unicast data in DPSK format. This is also known as OCS-DPSK format. One of the generated optical sub-carriers is

Authorized licensed use limited to: Chinese University of Hong Kong. Downloaded on July 26,2010 at 16:13:08 UTC from IEEE Xplore. Restrictions apply.

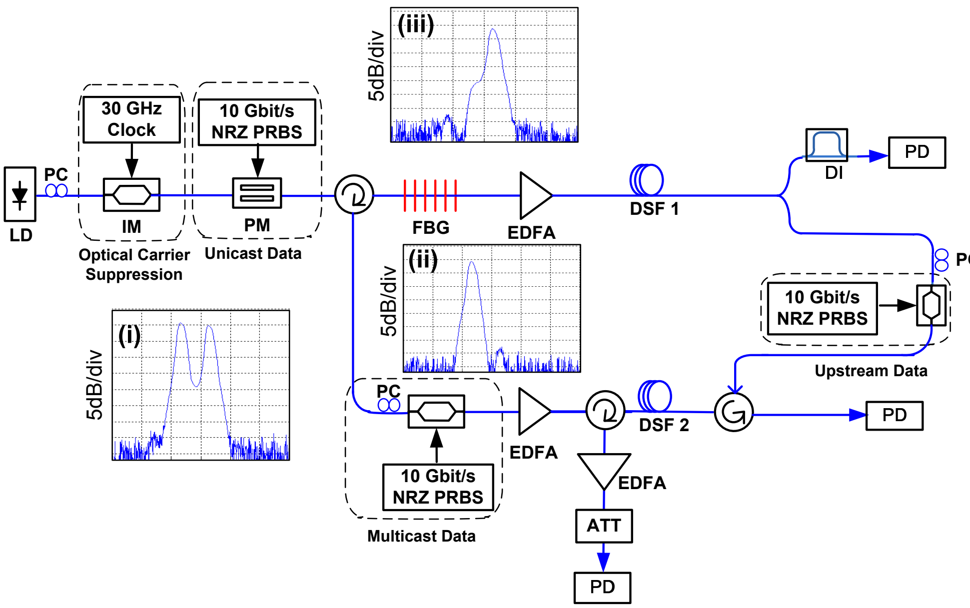

Fig. 3. Experimental setup. DSF: dispersion shifted fiber, PM: optical phase modulator, ATT: optical attenuator. Insets show the (i) output spectrum of the PM; (ii) reflected spectrum of FBG; (iii) transmitted spectrum of FBG. Horizontal scale: 0.5nm/div.

then filtered off and reflected, via a fiber Bragg grating (FBG). The reflected optical sub-carriers from all transmitters at the OLT are combined, via a WDM multiplexer, before being fed into a common IM for multicast ASK data modulation. The multicast composite signal is then delivered over the fiber feeder (F2) and demultiplexed at the remote node (RN) before being detected at their respective destined ONUs. On the other hand, the optical sub-carrier at the transmission output port of the FBG is transmitted to the respective ONU, via the fiber feeder (F1), to deliver the unicast data. At the RN, a typical $2 \times 2N$ array waveguide gratings (AWG), is employed. As illustrated in Fig. 1(b), its input ports are connected to the first and the second fiber feeders; while its i^{th} and $(N+i)^{th}$ output ports are connected to the same ONU$\#i$ ($i = 1, \ldots, N$), via separate distribution fibers. In this way, the downstream unicast wavelengths, from the first fiber feeder and the multicast wavelengths, from the second fiber feeder, can reach their respective destined ONUs. At each ONU, part of the received unicast DPSK data is demodulated, via an optical delay interferometer (DI), before direct detection. The rest of the downstream power is then fed into an IM for upstream ASK data modulation. The upstream signal is then transmitted, via the fiber feeder (F2), back to the respective receiver unit at the OLT. As the downstream unicast signal and the upstream signal are carried on different fiber feeders, while the upstream signal and the multicast signal are carried on different optical sub-carriers, though on the same fiber feeder, the possible Rayleigh backscattering effect is much alleviated.

The control of multicast transmission for individual downstream channel is achieved by turning on or off the control clock signal at the respective transmitter at the OLT. When the control clock is present, the optical sub-carrier for multicast data modulation is generated, hence multicast transmission is enabled. On the contrary, when the control clock is absent, the optical sub-carrier is no longer generated, thus there is no optical power available to carry the multicast data and disables the multicast transmission. The multicast control of all transmitters is performed at the OLT only.

Fig. 3 shows the experimental setup for the proposed scheme. A CW light at 1536.41 nm was first fed into a 40-Gb/s optical IM, driven by a 30-GHz clock to perform OCS and create two optical sub-carriers, λ_{sub1} at 1536.17 nm and λ_{sub2} at 1536.65 nm. The two optical sub-carriers were then phase modulated by a 10-Gbit/s $2^{31}-1$ pseudorandom binary sequence (PRBS) unicast data, via an optical phase modulator (PM), to generate OCS-DPSK signal. This procedure of OCS-DPSK signal generation could be simplified with a single IM, as suggested in Fig. 1, but a broadband electrical combiner was needed. These two methods of OCS-DPSK signal generation are alternatives and are technically equivalent. The OCS-DPSK signal,with a carrier suppression ratio of about 20 dB, as shown in Fig. 3 inset (i), was fed into an FBG with a reflection FWHM passband of 0.38 nm and a reflectivity of 99%, as depicted in Fig. 4, so as to separate the two optical sub-carriers. The optical sub-carrier, λ_{sub1}, as shown in Fig. 3 inset (ii), was reflected into another IM, where it was intensity modulated by the 10-Gbit/s $2^{31}-1$ PRBS multicast NRZ data and amplified to about 3 dBm before being fed into a piece of 20-km fiber feeder (DSF2). Dispersion-shifted fiber (DSF) was employed to emulate dispersion compensated links for the fiber feeders. At the transmission output port of the FBG, λ_{sub2}, as shown in Fig. 3 inset (iii), was amplified to about 5 dBm and delivered the downstream unicast DPSK data to the ONU, via another piece of 20-km fiber feeder (DSF1). At the ONU, the multicast data was directly detected. In addition, half of the received unicast DPSK signal power on λ_{sub2} is fed into an optical DI for demodulation and detection; while the other half was re-used as the upstream carrier, which was then

Authorized licensed use limited to: Chinese University of Hong Kong. Downloaded on July 26,2010 at 16:13:08 UTC from IEEE Xplore. Restrictions apply.

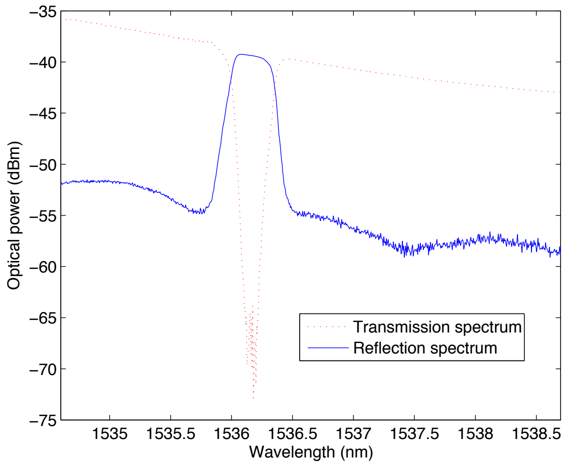

Fig. 4. Frequency response of the FBG.

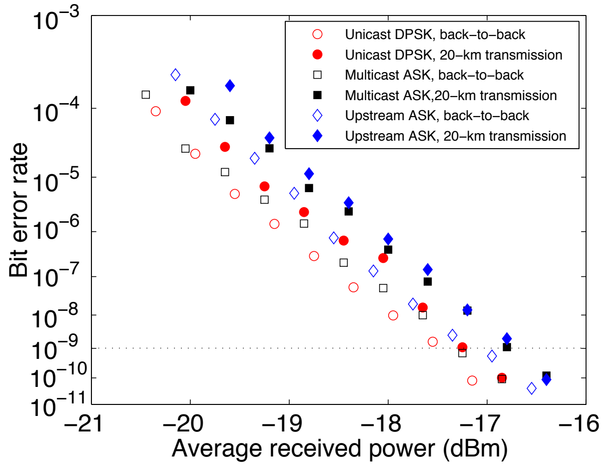

Fig. 6. BER measurements when multicast is enabled.

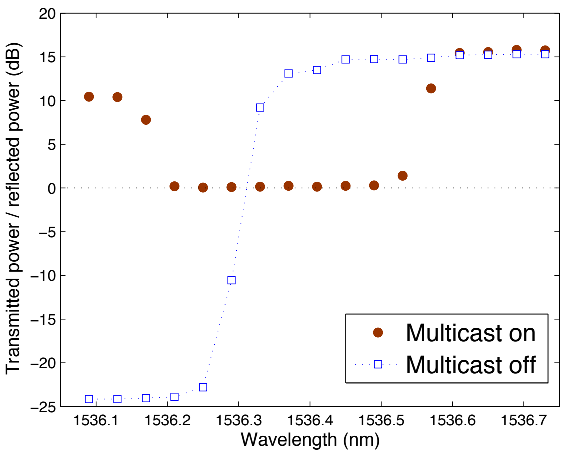

Fig. 5. Power ratio of the transmission power of the FBG over the reflective power of the FBG when the clock is 30 GHz.

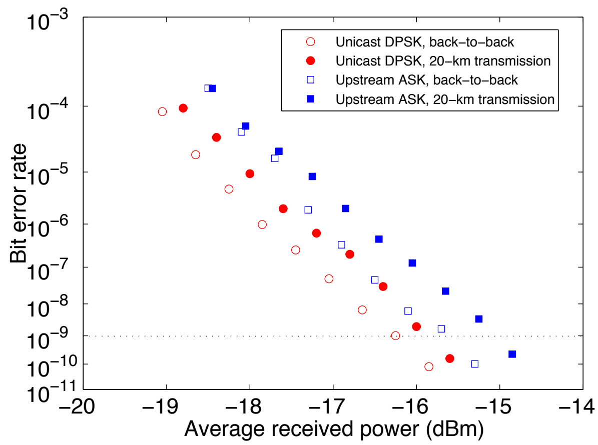

Fig. 7. BER measurements when multicast is disabled.

intensity modulated with the 10-Gb/s $2^{31}-1$ PRBS upstream NRZ data. The upstream ASK signal was then sent back to the OLT, via DSF2, for signal reception.

In order to characterize the performance of optical sub-carrier separation, via the FBG, we have measured the power ratio of the transmitted signal to the reflected signal of the FBG at the source wavelength, when the two optical sub-carriers generated from the source CW wavelength, via OCS with the presence of the 30-GHz clock (multicast-on) and the central carrier with the absence of the 30-GHz clock (multicast-off). The results were depicted in Fig. 5. When the source wavelength was set around 1536.41 nm, the power ratio was almost close to 0 dB under the multicast-on case, implying both of the separated optical sub-carriers were separated with similar intensity; while the power ratio was close to 15 dB under the multicast-off case, implying good suppression of the optical subcarrier for carrying the multicast signal.

Fig. 6 shows the measured bit-error-rate (BER) performances when the multicast was enabled by turning on the control clock signal to generate the optical sub-carrier for the multicast modulation. Less than 0.5-dB penalty was observed for the unicast, the multicast and the upstream data after transmission, showing receiver sensitivity (at BER $\leq 10^{-9}$) improvements by about 5 dB and 3 dB, for unicast and multicast transmissions, respectively, as compared with the previously reported approach [2]. Fig. 7 shows the BER performances when the multicast was disabled by turning off the control clock signal. The receiver sensitivities (at BER $\leq 10^{-9}$) for downstream unicast and upstream signals were degraded by 1.2 dB and 1.6 dB, respectively, after transmission, as compared with the multicast-enabled case. This could be attributed to the non-ideal reflection passband of the FBG, which induced excessive filtering to the central carrier when the control clock was absent, during which the wavelength of the downstream unicast DPSK signal will be closer to the reflection passband edge as shown in Fig. 2(b), as compared with when the multicast is enabled. This could be alleviated by employing a FBG with steeper edges in its reflective passband.

In our experiment, the optical power fed into the fiber feeder was about 3 dBm and 5 dBm for multicast and unicast signals, respectively. The losses caused by transmission, optical circulators and DI were around 5 dB, 1 dB, and 5 dB respectively. Thus, at the ONU, the optical power for

Authorized licensed use limited to: Chinese University of Hong Kong. Downloaded on July 26,2010 at 16:13:08 UTC from IEEE Xplore. Restrictions apply.

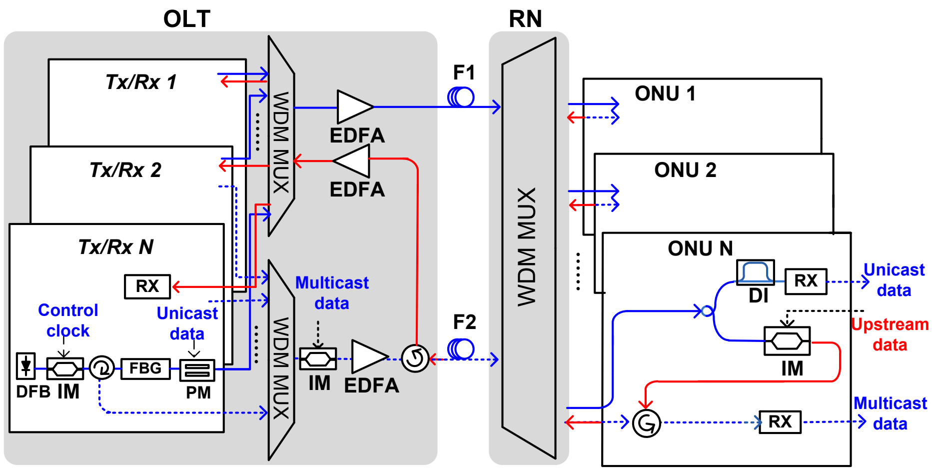

Fig. 8. A WDM-PON with modified multicast overlay scheme. F1 & F2: fiber feeders, FBG: fiber Bragg grating, IM: optical intensity modulator, EDFA: Erbium doped fiber amplifier, DI: delay interferometer.

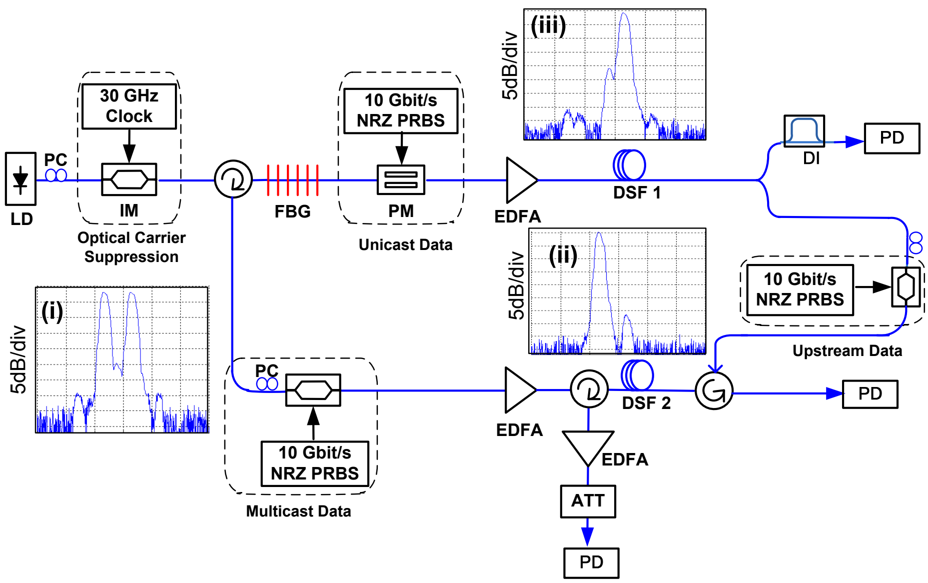

Fig. 9. Experimental setup of modified scheme. DSF: dispersion shifted fiber, PM: optical phase modulator, ATT: optical attenuator. Insets show the (i) output spectrum of the PM; (ii) reflected spectrum of FBG; (iii) transmitted spectrum of FBG. Horizontal scale: 0.5nm/div.

unicast data detection after DI was around -8 dBm, providing more than 9-dB system margin, while the optical power for multicast detection was around -3 dBm, implying around 14-dB system margin. Another portion of the unicast power was re-modulated at the ONU, via an IM, which induced about 6 dB insertion loss. Thus, the received optical power of the upstream signal at the OLT was around -15 dBm without amplification. However, by employing an optical amplifier before the WDM multiplexer at the OLT, the system could provide enough power margin for the upstream transmission. When considering the losses induced by the MUX/DMUX and RN in the multi-channel condition, extra 5 dB power loss has to be calculated. The optical power for unicast data detection after DI was around -13 dBm, providing more than 4-dB system margin, while the optical power for multicast detection was around -8 dBm, implying around 9-dB system margin. However, due to the optical amplifier employed in the upstream, the system could still provide enough power margin for the upstream transmission. In our experiment, only one channel was considered to demonstrate the operational features and the proof-of-concept of our proposed scheme. For the more realistic scenario of multiple channels in the network, there may be possible crosstalk among the channels which induces power penalty to individual channels. Therefore, it is crucial to assure enough system margin to cope with such possible crosstalk-induced power penalty in practical system design.

III. Modified Optical Multicast Overlay Scheme

Fig. 8 depicts a modified multicast WDM-PON architecture with N ONUs and the modifications are made at the OLT. Basically, at each transceiver of the OLT, the unicast data is modulated onto the generated optical sub-carriers at the output of FBG, via an optical phase modulator, instead. In

Authorized licensed use limited to: Chinese University of Hong Kong. Downloaded on July 26,2010 at 16:13:08 UTC from IEEE Xplore. Restrictions apply.

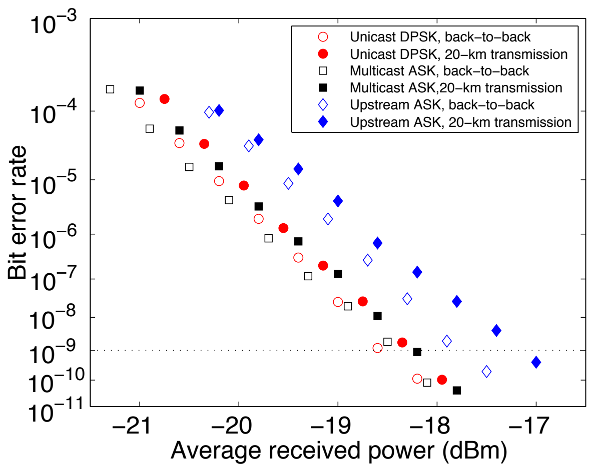

Fig. 10. BER measurements when multicast is enabled, for the modified scheme.

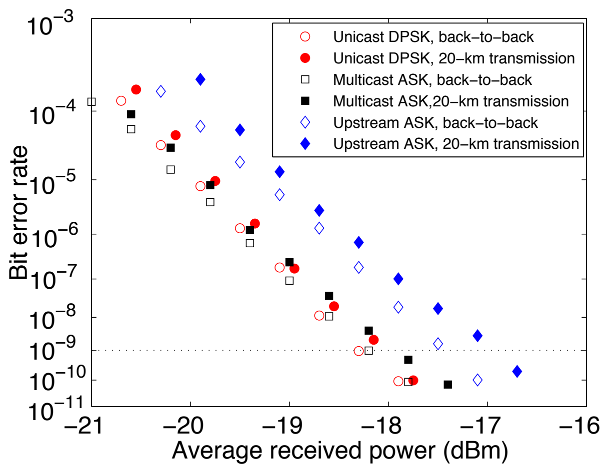

Fig. 12. BER measurements with multicast enabled when the control clock frequency is 20-GHz.

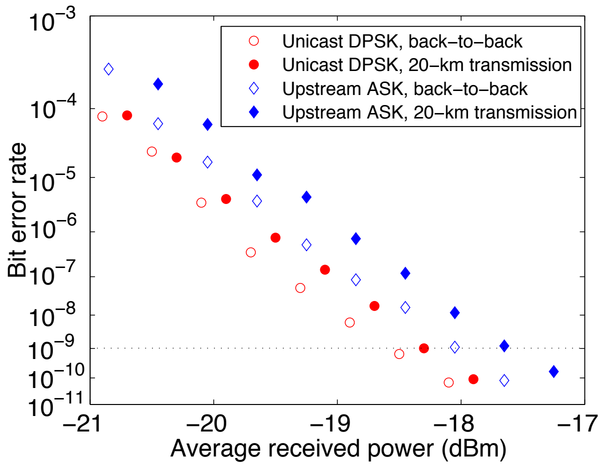

Fig. 11. BER measurements when multicast is disabled, for the modified scheme.

this way, the non-ideal frequency response of the FBG will bring less phase-to-intensity noise to not only the multicast data but also the unicast data as well as the upstream data compared with the scheme shown in Fig. 1. This is attributed to the fact that phase modulation broadens the spectrum of the signal. When the phase modulation is performed before the FBG filtering, as in Fig. 1, the non-ideal frequency response of the FBG may convert the phase information into amplitude fluctuation, which deteriorates the signal performance. Such phase-modulation induced spectral broadening also reduces the optical carrier suppression ratio during the OCS process, and thus hinders the optical sub-carrier separation through the FBG. With the modified scheme, these impairments can be alleviated and thus leads to improvement in the system performance as well as relaxed requirement in the control clock frequency.

We have measured the BER performance to verify this possible improvement, using the experimental setup as shown in Fig. 9. Fig. 10 shows the measured BER performances with the presence of the 30-GHz control clock signal so as to generate the optical sub-carrier for the multicast modulation. At BER $\leq 10^{-9}$, less than 0.3-dB penalty was observed for both the unicast and the multicast data, while about 0.5-dB penalty was observed for the upstream data after 20-km transmission. As compared with the measurements of the original scheme depicted in Fig. 6, the measured receiver sensitivities (at BER $\leq 10^{-9}$) of the downstream multicast, the downstream unicast and the upstream transmissions, were improved by about 1.3 dB, 1 dB, and 0.8 dB, respectively, after transmission. They were mainly attributed to the phase-to-amplitude conversion noise due to crosstalk of DPSK to ASK signal and the better filtering effect of FBG without the spectrum broadening via the phase modulation. Fig. 11 shows the BER performances with the absence of the control clock signal, thus the multicast transmission was disabled. As compared with the measurements of the original scheme depicted in Fig. 7, the receiver sensitivities (at BER $\leq 10^{-9}$) for the downstream unicast and the upstream signals were improved by 2.3 dB, and 2.5 dB, respectively, after transmission. This larger improvement compared with multicast-enabled case was mainly attributed to the fact that the central optical carrier was closer to the non-ideal reflection edge of the FBG when the control clock was absent, thus would suffer from much more severe excessive filtering at the FBG.

In the experiment of the modified scheme, the optical power fed into the transmission link was about 3 dBm and 5 dBm for the multicast and the unicast signals, respectively. The losses caused by transmission, optical circulators and DI remained the same as in the original scheme. Thus the system margin for the unicast and the multicast transmissions were improved by 1 dB, to around 10 dB and 15 dB, respectively. While the system margin for upstream transmission was also improved by about 0.8 dB.

IV. Control Clock Frequency Requirement and Residual Rayleigh Backscattering Effect

In the modified scheme, we have investigated the performances when the frequency of the control clock at the OLT are reduced to 20 GHz as well as 15 GHz. Fig. 12 shows the measured BER performances when the multicast transmission was

Authorized licensed use limited to: Chinese University of Hong Kong. Downloaded on July 26,2010 at 16:13:08 UTC from IEEE Xplore. Restrictions apply.

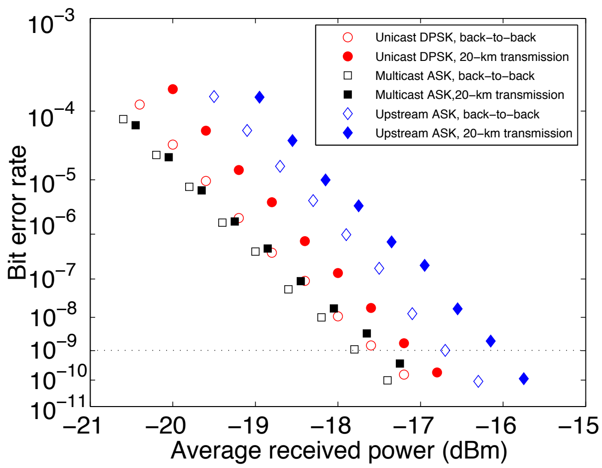

Fig. 13. BER measurements with multicast enabled when the control clock frequency is 15-GHz.

enabled with the presence of the 20-GHz control clock. The receiver sensitivities after 20-km transmission were degraded by about 0.2 dB and 0.3 dB, for the downstream and the upstream transmissions, respectively, as compared with that when the clock was 30-GHz, as depicted in Fig. 10. These negligible degradations might be attributed to the slight reduction (from 23 dB to 21 dB) in the optical carrier suppression ratio. Fig. 13 shows the BER performances when we set the control clock frequency to 15-GHz. The receiver sensitivities (at BER $\leq 10^{-9}$) for the downstream unicast and multicast signals were deteriorated by 1.1 dB and 0.6 dB, respectively, after transmission, while about 1.3-dB degradation was observed for the upstream signal, as compared with that depicted in Fig. 10. These larger degradations might be attributed to the larger reduction (from 23 dB to 15 dB) in the optical carrier suppression ratio when the control clock frequency was 15 GHz. The closer spacing between the two optical sub-carriers would induce more noises due to phase-to-amplitude conversion at the FBG, and induced more degradation to the upper optical sub-carrier than the lower optical sub-carrier.

As shown in Fig. 8, the system architecture guarantees no Rayleigh backscattering (RB) effect in the feeder fibers, as the upper feeder fiber has only uni-directional signal transmission, while the lower one has bi-directional signal transmissions, but on different wavelengths. However, in practice, due to non-ideal separation of the two generated optical sub-carriers at the OLT, the residual spectra might lead to possible wavelength overlapping or crosstalk in the lower feeder fiber. This wavelength overlapping between the optical sub-carriers would introduce possible RB. We have characterized such residual RB in our experiment under three values of the control clock frequency at the OLT, and the results were tabulated in Table 1. The residual RB for all the three conditions were less than 0.32 dB, for both the multicast and the upstream transmissions, which implied negligible RB in our scheme. This was due to the relatively low power in the wavelength overlapping component.

TABLE I
RESIDUAL RAYLEIGH BACKSCATTERING.

Control clock frequency at OLT	Rayleigh Backscattering (dB)	
	Upstream	Multicast
15 GHz	0.32 dB	0.30 dB
20 GHz	0.30 dB	0.28 dB
30 GHz	0.28 dB	0.25 dB

V. SIMULTANEOUS TRANSMISSION OF TWO SETS OF MULTICAST DATA

In this section, we extend our scheme to realize simultaneous multicast transmission of two sets of data streams over a WDM-PON. Fig. 14 depicts the WDM-PON with an optical overlay scheme to support two sets of multicast data. Compared with the scheme, illustrated in Fig. 8, we further superimpose the second set of multicast data in DPSK format (multicast data 2), via orthogonal modulation technique, onto the first set of multicast data in ASK format (multicast data 1). An additional PM is employed after the multicast IM modulator so as to support modulation of the second set of multicast data in DPSK format. In order to realize the simultaneous transmissions of the two multicast data, we add an electrical attenuator and switch to control the extinction ratio (ER) of the multicast data 1. When the ER of the multicast data 1 (ASK), is reduced, the multicast data 2 (DPSK) modulated on the multicast data 1 (ASK) can be successfully demodulated and thus simultaneous transmission is enabled. On the other hand, when the ER of the multicast data 1 is set to be higher than 4.7 dB [12], the multicast data 2 (DPSK) modulated on the multicast data 1 (ASK), can no longer be properly demodulated at the ONU, due to the excessive induced intensity fluctuation, thus multicast data 2 is disabled.

Fig. 15 shows the BER performances when single multicast (either multicast data 1 or 2) was enabled. After 20-km transmission, the power penalties were about 0.4 dB for the downstream unicast transmission and 0.6 dB for both the downstream multicast and the upstream transmissions. Fig. 16 shows the BER performances when simultaneous double multicast (both multicast data 1 or 2) was enabled. As compared to the results shown in Fig. 15, about 5 dB and 5.5 dB reduction in the receiver sensitivities (at BER $\leq 10^{-9}$) were shown for the multicast DPSK signal (multicast data 2) and the multicast ASK signal (multicast data 1), respectively. The relatively large performance degradation in multicast data 1 (ASK) might be attributed to reduction of its ER from 8.5 dB to 3.1 dB in the experiment, while that in multicast data 2 (DPSK) might be due to the intensity fluctuation induced from multicast data 1 (ASK). However, the simultaneous transmissions of the two sets of multicast data had negligible degradation on both the downstream unicast and the upstream data.

VI. SUMMARY

We have proposed and experimentally investigated a novel optical multicast overlay scheme for WDM-PONs, so as to enhance the networking flexibility. It is based on optical carrier suppression technique to generate the optical sub-carrier

Authorized licensed use limited to: Chinese University of Hong Kong. Downloaded on July 26,2010 at 16:13:08 UTC from IEEE Xplore. Restrictions apply.

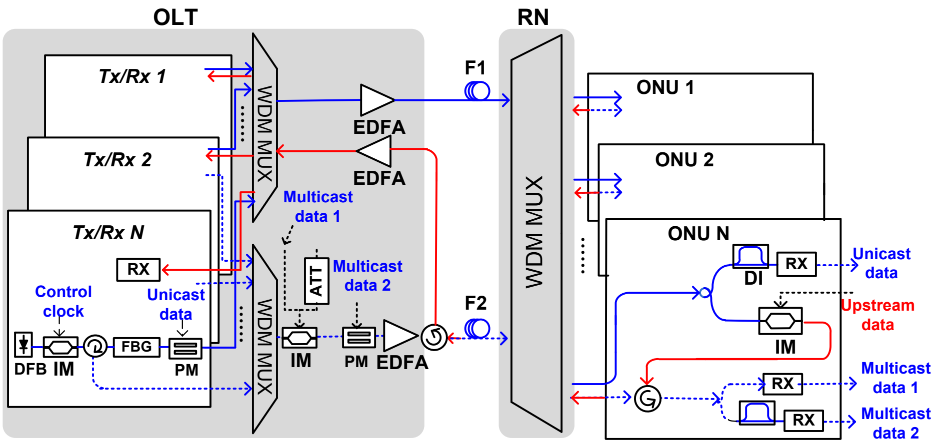

Fig. 14. A WDM-PON with an overlay scheme to realize simultaneous transmission of two sets of multicast data. F1 & F2: fiber feeders, FBG: fiber Bragg grating, IM: optical intensity modulator, EDFA: Erbium doped fiber amplifier, DI: delay interferometer.

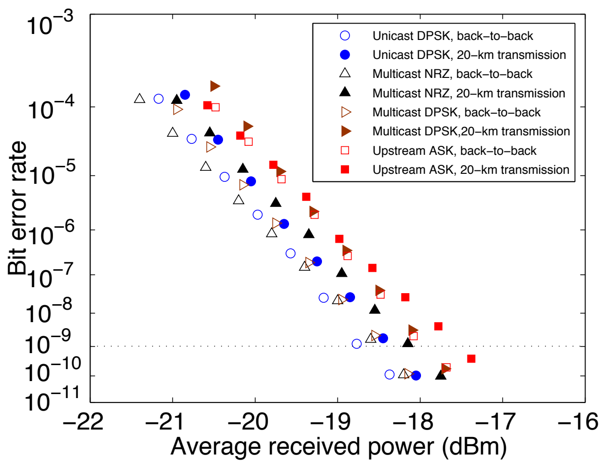

Fig. 15. BER measurements when single multicast data stream is enabled.

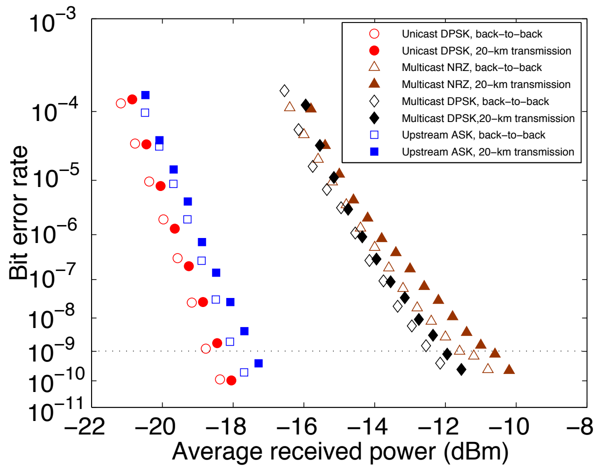

Fig. 16. BER measurements when two multicast data streams are enabled.

for the multicast data modulation. Simple multicast overlay control is performed by setting the presence of the control clock signal at the OLT. Simultaneous 10-Gb/s transmissions of the downstream unicast and multicast data, as well as the upstream data have been demonstrated with satisfactory system performance. Moreover, we have further modified the scheme to alleviate the possible degradation due to phase-to-intensity conversion at the non-ideal passband edge of the FBG at the OLT. Furthermore, the requirement of the control clock frequency for OCS, as well as the possible RB in the system, have been experimentally characterized. In addition, we have also successfully demonstrated the simultaneous transmission of two sets of multicast data over the WDM-PON, using orthogonal modulation technique.

References

[1] N. Deng, C. K. Chan, L. K. Chen and C. Lin, “A WDM passive optical network with centralized light sources and multicast overlay,” *IEEE Photon. Technol. Lett.*, vol. 20, no. 2, pp. 114-116, 2008.

[2] Y. Zhang, C. K. Chan, and L. K. Chen, “A multicast WDM-PON architecture using DPSK/NRZ orthogonal modulation,” *IEEE Photon. Technol. Lett.*, vol. 20, no. 17, pp.1479-1481, 2008.

[3] J. Xu, C. K. Chan, and L. K. Chen, “A WDM-PON with 10-Gb/s symmetric bit-rates and multicast overlay with delay-based multicast control,” *IEEE/OSA Optical Fiber Communication Conference / National Fiber Optic Engineers Conference , (OFC/NFOEC)*, Paper NME5, San Diego, USA, Mar. 2009.

[4] L. Cai, Z. Liu, S, Xiao, M. Zhu, R. Li and W. Hu “Video-service-overlaid wavelength-division-multiplexed passive optical network,” *IEEE Photon. Technol. Lett.*, vol. 21, no. 14, pp. 990-992, 2009.

[5] M. Khanal, C. J. Chae, and R. S. Tucker, “Selective broadcasting of digital video signals over a WDM passive optical network,” *IEEE Photon. Technol. Lett.*, vol. 17, no. 9, pp. 1992-1994, 2005.

[6] Q. J. Chang, J. M. Gao, Q. Li, and Y. K. Su, “Simultaneous transmission of point-to-point data and selective delivery of video services in a WDM-PON Using ASK/SCM Modulation Format,” *IEEE/OSA Optical Fiber Communication Conference / National Fiber Optic Engineers Conference (OFC/NFOEC)*, Paper OWH2, San Diego, California, USA, 2008.

[7] Y. Tian, Q. J. Chang, and Y. K. Su, “A WDM passive optical network enabling multicasting with color-free ONUs,” *OSA Opt. Express*, vol. 16, no. 14, pp. 10434-10439, Jul. 2008.

[8] Y. Qiu and C. K. Chan, “A WDM passive optical network with polarization-assisted multicast overlay control,” *IEEE Photonics Technol. Lett.*, vol. 21, no. 16, pp. 1133-1135, 2009.

[9] Y. Qiu and C. K. Chan, “A simple multicast overlay scheme for WDM passive optical networks with symmetric two-way traffic,” *OptoElectronics and Communications Conference (OECC)*, Paper WT1, Hong Kong, Jul. 2009.

[10] Y. Qiu and C. K. Chan, “A novel multicast overlay scheme for WDM passive optical networks using optical carrier suppression technique,”

Authorized licensed use limited to: Chinese University of Hong Kong. Downloaded on July 26,2010 at 16:13:08 UTC from IEEE Xplore. Restrictions apply.

European Conference on Optical Communications (ECOC), Paper P6.14, Vienna, Austria, Sep. 2009.

[11] O. Akanbi, J. Yu and G. K. Chang, "A new scheme for bidirectional WDM-PON using upstream and downstream channels generated by optical carrier suppression and separation technique," *IEEE Photonics Technol. Lett.*, vol. 18, no. 2, pp. 340-342, 2006.

[12] M. Ohm and J. Speidel, "Quaternary optical ASK-DPSK and receivers with direct detection," *IEEE Photon. Technol. Lett.*, vol. 15, no. 1, pp. 159-161, Jan. 2003.

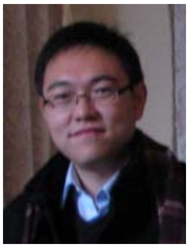

Yang Qiu received the B.Sc. degree in Communication and Information Engineering from University of Electronic Science and Technology of China, Chengdu, China, in 2005. Currently, he is pursuing his Ph.D. degree in Information Engineering at the Chinese University of Hong Kong. His research interests include optical communications and optical access networks.

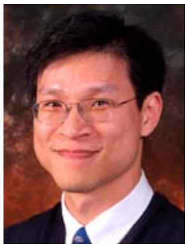

Chun-Kit Chan (S'93-S'95-M'97-SM'04) received the B.Eng., M.Phil., and Ph.D. degrees from The Chinese University of Hong Kong, Hong Kong, all in Information Engineering. In 1997, he joined the Department of Electronic Engineering, City University of Hong Kong, as a Research Assistant Professor. In 1999, he joined Bell Laboratories, Lucent Technologies, Holmdel, NJ, as a Member of Technical Staff, where he worked on control of widely tunable semiconductor lasers and realization of an optical packet switch fabric with terabit-per-second capacity. In August 2001, he joined the Department of Information Engineering, The Chinese University of Hong Kong, where he is currently an Associate Professor. He has served as the member of the technical program committee for OFC/NFOEC and a number of other international conferences. He has published more than 180 technical papers in refereed international journals and conference proceedings, one edited book and two book chapters. He holds one issued U.S. patent. Currently, he serves as the Associate Editor of *IEEE/OSA Journal of Optical Communications and Networking*. His main research interests include optical access networks, optical packet switching, and optical performance monitoring.

Authorized licensed use limited to: Chinese University of Hong Kong. Downloaded on July 26,2010 at 16:13:08 UTC from IEEE Xplore. Restrictions apply.